Supplementary Information
for

Increasing Concurrence of Wildfire Drivers Tripled Megafire Critical Danger Days in Southern California

by

Mohammad Sadegh Khorshidi, Philip E. Dennison, Mohammad Reza Nikoo, Amir AghaKouchak, Charles H. Luce, Mojtaba Sadegh

S1. Methods:

S1.1. Live fuel moisture (LFM) is the mass of water within a vegetation sample divided by the dry mass of the sample. Chamise (*Adenostoma fasciculatum*) is an evergreen shrub species commonly found throughout California chaparral (Hanes, 1977). Dennison and Moritz (2009) demonstrated that as chamise LFM declines, a critical threshold is reached below which large fire activity occurs. This threshold has recently been shown to coincide with leaf turgor loss point (Pivovaroff et al. 2019). Southern California fire departments and federal agencies operate an extensive network of LFM sampling sites, with 51 sites (Fig. S1) and 8,255 chamise LFM samples within our study region between 1992 and 2015 (total of 9,680 available chamise LFM samples between 1983 and 2017; National Fuel Moisture Database). The time interval between about 65 percent of the successive records provided by NFMD is within 20 days (Fig. S8). We used spline interpolation to determine LFM on the discovery date of each fire, limiting the time between LFM samples to a maximum of 15 days. The temporally interpolated LFM value closest to the location of the fire record was then assigned to that fire (Dennison and Moritz, 2010).

S1.2. Wind speed plays a crucial role in spreading fires, especially in regions with extensive fine fuels like Southern California. Coastal Santa Barbara County experiences northerly katabatic winds referred to as Sundowners, while the remainder of the study area is exposed to easterly and northeasterly katabatic winds termed Santa Ana winds. Santa Ana winds are most common from late fall to early winter (Raphael, 2003). Very low relative humidity during katabatic wind events desiccates dead fuels and increases vapour pressure deficit. We used a spline interpolation method to estimate the average wind speed during the first 48 hours from the discovery time of each fire (or the entire duration of the fire, whichever was shorter) at the closest grid cell center to the fire location, using the North American Regional Reanalysis' 3-hourly 10 m above ground wind speed at 32-km resolution. We acknowledge that the spatial resolution of wind data can introduce a level of uncertainty to our analysis as this does not capture local topographic roughness impacts.

S1.3. 3-day Standardized Heatwave Index (SHI3) is a statistical metric of temperature anomaly introduced by Raei et al. (2018), which is based on a z-score of the average 3-day mean temperature for the target day with respect to the distribution of the observed mean daily temperatures in a period of one week before and after the target day in a 30+ year climate record. Various studies have shown the impact of increased temperature on wildfire activity. Moreover, Jolly et al. (2015) demonstrated the impact of heatwaves on increased global wildfire activity. Here, we used Parameter-elevation Regressions on Independent Slopes Model (PRISM)'s daily temperature at 4-km resolution to derive gridded 3-day SHI between 1982 - 2018. The SHI value of the center of the grid cell closest to the fire location on the discovery date was assigned to each fire.

S1.4. 100- and 1000-hour Dead Fuel Moisture (FM100 and FM1000, respectively), Energy Release Component (ERC) and Burning Index (BI) are fire danger metrics introduced by U.S. National Fire Danger Rating System (NFDRS; Deeming, 1977) to determine fire potential. FM100 and FM1000 indicate the moisture content of dead fuels with diameters 2.5-7.6 cm (1-3 inches) and 7.6-20.3 cm (3-8 inches), respectively. Hour values in FM100 and FM1000 represent time lags for a decay function that brings the fuel elements to equilibrium with ambient relative humidity. ERC is a weather-climate proxy derived from temperature, precipitation, solar radiation and relative humidity, and represents the amount of available energy at the flame front of a fire; whereas BI is a metric incorporating ERC and wind speed.

S1.5. Vapour Pressure Deficit (VPD) is the difference between the air's actual and saturation vapour pressure, and indicates evaporative demand and stress on live vegetation. Williams et al. (2015) found that VPD is one of the dominant indicators of fire activity in the southwestern U.S. We used GridMET's (Abatzoglou, 2013) daily FM100, FM1000, ERC, BI, and VPD gridded data at 4-km resolution for our study. The values of closest grid cell center to the location of fire on the discovery date was assigned to each fire.

S2. Tables and Figures

Table S1. Detailed literature review. Scope of each study, method, and the findings are presented. Findings are often quotes from the original paper.

Reference	Region	Fire Size Threshold	Years of Fire Record	Drivers*	Goal of Study (Modified Quote from the Source)	Result (Modified Quote from the Source)
Bessie and Johnson 1995	Subalpine Forests	-	1954-1988	FM100, FM1000, TEMP, PREC, WS, RH	Impact of weather and fuel on fire intensity and crown fire initiation	Fire characteristics are strongly correlated with weather and fuel moisture
Westerling et al. 2003	western U.S. (Bailey's ecosystem)	Gridded data	1983-2000	PDSI	- Wildfire frequency and area burned in the western U.S. - Relationships between PDSI and abnormal fire activity	- Moisture anomalies are correlated to abnormal summer fire activity in Western U.S. - Area burned in shrub and grasslands are strongly dependent on fuel accumulation and antecedent climate conditions.
Brown et al. 2004	western U.S.	>40 ha (or the fires with more than 750,000$ suppression cost)	1980-2000	ERC	Project wildfire changes in Western U.S. in 21st century.	From 2070, CO2 will increase two folds and ERC will exceed the 60 threshold in two to three weeks.
Westerling et al. 2006	western U.S.	>400 ha	1970-2003	TEMP, SDA and MD	Extent of climate impact on recent change in wildfire activity	Large wildfire activity increased from mid-1980s and it is associated with earlier snowmelt and increase in spring and summer temperature.
Westerling and Bryant 2008	California	>200 ha	1980–1999	EL, PREC, TEMP, SM, and SWE	Project wildfire risks for California under climatic change scenarios	Increased temperature promotes greater large fire frequency in some regions, while in other regions, lower precipitation and higher temperature reduce fine fuel availability and reduce fire risks.
Spracklen et al. 2009	Western U.S. ecosystems (Bailey et al. 1994)	>400 ha	1970-2003	TEMP, RH, WS, PREC, FMC, and FSI.	Climate change impact on wildfire activity carbonaceous aerosol concentrations in the western U.S.	Higher temperature increases annual mean area burned. Consequently, increased area burned will double carbonaceous aerosol emissions by midcentury.
Littell et al. 2009	Western U.S. ecoprovinces (Bailey et al. 1994)	>405 ha	1916-2003	PREC, TEMP, and PDSI	Impact of climatic variables on the area burned in different vegetation types in the western U.S.	Area burned by wildfires are controlled by climate, despite fire suppression and fuel treatment practices. High temperature, low precipitation and PDSI promotes increased area burned.
Dennison and Moritz 2009	LA County	>1000 ha	1981–2006	PREC to determine critical LFM	Determine critical live fuel moisture for large fires.	The critical LFM threshold for LA County is 79%. The timing of this threshold is correlated with antecedent rainfall. Lower spring precipitation causes LFM decline in fire season, while higher winter precipitation could delay the timing of LFM threshold.
Liu et al. 2010	Global	-	-	KBDI	Project trend of global wildfire potential under climate change	Fire potential escalates in the U.S., South America, central Asia, southern Europe, southern Africa, and Australia, and fire season becomes longer. The main drivers of more fire activity is warming and dryness.
Abatzoglou and Kolden 2011	Western U.S. deserts	-	-	ERC, TEMP, RH, PREC, WS, and state of the weather	Changes in temperature thresholds, the timing and availability of moisture, large wildfires potential under climate projections	Increased fire season and frequency in winters will alter vegetation cover and establishes invasive grasses. This will cause more lengthening of fire season in a feedback loop.
Westerling et al. 2011a	California	>200 ha	1980-1999	TOPO, TEMP, PREC, WS, MD, RH, SM, SWE and vegetation type	Hydroclimate and landsurface to predict large wildfire and burned area	Increases are predicted in wildfire burned area which is risen with higher emissions pathway.
Westerling et al. 2011b	Greater Yellowstone ecosystem	>200 ha	1972-1999	TOPO, TEMP, PREC, WS, MD, RH, SM, SWE and vegetation type	Climate controls on large fires occurrence, size, spatial location	Noticeable fire increases were predicted by all models by mid-century
Abatzoglou and Kolden 2011	Alaska	>1200 ha	1980-2007	TEMP, PREC, WS, and RH	Impact of higher-frequency weather and lower-frequency climate on fire increases in Alaskan.	Increased freeze fire season and frequency in winters will alter vegetation cover, and favours cold-intolerant annual grasses and establishes invasive grasses. This will cause more lengthening of fire season in a feedback loop.
Holden et al. 2011	Pacific Northwest U.S.	>400 ha	1984-2005	snowmelt-induced streamflow timing and total annual streamflow	Correlation of total area burned and its severity to snowmelt-induced streamflow timing and total annual streamflow metrics.	Correlations of burned area and streamflow and its timing are significant. Area burned variability, which previously attributed solely to temperature, is primarily driven by precipitation and streamflow.
Dillon et al. 2011	Western U.S. (ecoregions,)	>405 ha	1984-2006	TOPO, TEMP, PREC, and SM	Influence of topography, weather and climate on fire severity	The degree of fire severity is influenced by topography, which is more impressive predicator, than weather and also climate.
Finney et al. 2011	Continental U.S.	-	-	ERC, WS	Probabilistic wildfire risk assessment for the continental U.S.	Fire size distribution can be determined by joint distributions of fire growth and conducive weather sequences opportunities.
Parisien et al. 2012	Western U.S.	All fires from MTBS and Landfire	1984-2008	FD, population, TOPO, WS, PREC, TEMP, density of lightning strikes, and primary productivity	High-resolution estimates of wildfire probability.	Wildfire probabilities is not uniform, and its response to environmental variables differs spatially. Humans are the main cause of wildfire activity.
Liu et al. 2013	Entire U.S.	-	-	KBDI and FFWI	Impact of climate change on wildfire potential trends in the continental U.S.	Fire potential have increased in recent decades. Based on projected KDBI, the same trend is expected for future. Larger fire potential variability is also expected for Pacific and Atlantic coastal regions.

Luo et al. 2013	Western U.S.	-	-	HI	Speed of wildfire growth under changing climate	The projections predict more days and more successive days with increased risk for rapid wildfire growth. More erratic wildfires are expected in mountainous regions of western U.S.
Yue et al. 2013	Western U.S.	>10 ha	1980-2004	TEMP, RH, WS, RH, WS, PREC, FMC and FSI.	Project wildfire activity during 2046-2065	Significant increases in future area burned, length of fire season and carbon emissions from wildfires are predicted.
Flannigan et al. 2013	Global	-	-	CSR	Climate change impact on global fire season severity and length in mid-century (2041–2050) and late century (2091–2100)	Significant increases for CSR and fire season length are predicted. The largest increase is predicted for Northern Hemisphere at the end of the century.
Abatzoglou and Kolden 2013	Western U.S.	>404 ha	1984–2010	PREC, TEMP, PDSI, SWE, SM, ERC, BI, FM100, FM1000, MD, CWD, FFMC, DMC, and Drought Codes.	Large-scale climate–fire relationships in the western U.S.	Fuel and soil moisture have stronger correlations to area burned than climate variables antecedent to fire season. Biophysical variables are better describers of wildfire activity than standard climate variables.
Riley et al. 2013	Western U.S.	>405 ha	1984-2005	ERC, PREC, PDSI, and SPI	Correlations between drought and firedanger-rating indices	Both area burned and fire frequency are strongly correlated with percentiles of short-term Energy Release Component and monthly rainfall. However, long-term Energy Release Component, monthly rainfall, Palmer Drought Severity Index and 24-month Standardized Precipitation Index percentiles are weakly correlated with those metrics.
Barbero et al. 2014	Contiguous U.S. (Omernik level II ecoregions)	>404 ha	1984-2010	TEMP, RH, ERC, BI, ISI, FFWI, PREC, PDSI, and CWD.	Model very large-fire (>5000 ha) occurrences probability over the continental U.S. from weather and climate forcing	Above normal wet condition during growing seasons conducive to very large fires (VLF) increases the probability of VLFs in interannual timescales in rangelands while long-term droughts are the main driver of VLFs in forests. In short-term, fire weather is the main driver of VLFs in rangelands while dead fuel moisture is the main driver of VLFs in forests.
Stavros et al. 2014	Contiguous western U.S. (Geographic Area Coordination Centers (GACC))	>404 ha	1984–2010	PDSI, TEMP, FFMC, DMC, FM100, FM1000, ERC, and BI.	Project seasonal changes in the climatic potential for very large wildfires (VLWF≥50,000 ac~20,234 ha)	Both RCP 4.5 and 8.5 projections show significant increase of very large fire (VLF) probability for mid-21st century.
Dennison et al. 2014	Cestern U.S. (Omernik level III ecoregions)	>405 ha	1984–2011	TEMP, PREC, and PSDI	Regional trends in fire occurrence, total fire area, fire size, and day of year of ignition for 1984–2011	The trend of large fire frequency and annual burned area is abruptly increasing during 1984 to 2011.
Jin et al. 2014	Southern California	>40 ha	1959-2009	TEMP, PREC, DP, RH, WS, and PDSI	Controls on wildland fires in Southern California during periods with and without Santa Ana winds	Models roughly explained seasonal and interannual number of Santa Ana and non-Santa Ana fires. Santa Ana fires' frequency increased during the years with lower relative humidity and fall rainfall. Cumulative rainfall during three winter conducive to fires are strongly correlated with the number of non-Santa Ana fires. The number of extremely large Santa Ana fires is substantially increased in the past decade.
Jolly et al. 2015	Global	-	1979-2013	BI, CFWI, and AFFDI.	Metric of fire weather season length, and map spatio-temporal trends from 1979 to 2013	Fire weather season have lengthened across the globe. This lengthening is responsible for doubling of burned area during 1979 to 2013.
Barbero et al. 2015a	Eastern U.S.	>202 ha	1984-2010	PDSI, ERC, and FFWI	Relationships between climatic conditions and the occurrence of very large-fires (VLF, >3000 ha) in the Eastern U.S.	Very large fires (VLF) are mostly occur after a long-term drought and during a sub-seasonal drought through low fuel moisture and lengthened fire-weather season.
Barbero et al. 2015b	Contiguous U.S.	-	-	Follow up for Barbero et al. 2014.	- Model very large fires (VLFs; Barbero et al. 2014) (>5000 ha), - Ensemble of 17 global climate models: VLF occurrence arising from anthropogenic climate change	In the regions with most historic fire activity, the projections show the most increase in very large fires occurrence, burned area and season. The regions with most increase are Northern California and intermountain West.
Williams et al. 2015	Southwest U.S. (forests)	-	1984–2013	PREC, TEMP, VPD, PET, MD, WS, SM, PDSI, KDBI, SPEI, and ERC	Correlations between components of the water balance and burned area in the southwest U.S. forests	- . Fifteen metrics are strongly correlated with annual burned area within forests, which causes more complication to accurately predict burned area. One of these metrices is spring and summer vapor pressure deficit. If an aggressive emission pathway is taken into consideration, vapor pressure deficit would exceed its highest record by 40% in the current mid-century.
Westerling 2016	Western U.S. (forests)	>400 ha	1970–2012	TEMP, SDA and MD	Sensitivity of western U.S. forests to changes in timing of Spring snowmelt	Wildfire frequency and burned area increased over the past two decades in both forests and non-forest areas across western U.S.. wildfire activity is strongly correlated with warming and earlier spring snowmelt.
Abatzoglou and Williams 2016	Western U.S. (forests)	>404 ha	1984–2014	ETo, VPD, CFWI, ERC, CWD, AFFDI, KBDI and PDSI	Modelled climate projections to estimate the contribution of anthropogenic climate change to observed increases in eight fuel aridity metrics and forest fire area across the western U.S..	Fuel aridity is increased by anthropogenic climate change in forests of western U.S. in the past decades. Both fire season length and activity in the region is affected by climate change.
Abatzoglou et al. 2016	Western U.S.	-	1992-2013	Cloud to ground lightning, ERC, VPD, PREC, and PDSI	Controls on interannual variability in lightning-caused fire activity	The number of lightning strikes shows strong correlation with interannual fire frequency; however, it is poorly correlated with annual area burned. On the other hand, climatic conditions are strongly correlated with annual area burned.
Schoennagel et al. 2017	Western U.S. (forests)	-	-	-	An approach that accepts wildfire as an inevitable catalyst of change and promotes adaptive responses by ecosystems and residential communities to more warming and wildfire	This study shows that reduction of fuels and current fuel treatment practices does not reduce wildfire activity. Thus, new approaches should be adopted to adapt residential communities and ecosystems to more wildfire activity.
Taufik et al. 2017	Borneo	Gridded data	1996-2015	Groundwater recharge	Impact of hydrological droughts on wildfire activity	Hydrological processes and data are more reliable forcing compared to climatic data for models predicting burned area.
Balch et al. 2017	U.S.	>405 ha	1992-2012	Monthly lightning density, FM1000	Role of human activity on wildfires in U.S.	Overall human-cause fire season is longer than lightening-cause season. Humans' activity substantially increased fire frequency and burned area over the 21-year time span. Humans ignited fires account for 5.1 million km^2 while lightening ignited fires caused only 0.7 million km^2 in the same period.
Chikamoto et al. 2017	North America	Not used	-	FD, SWC, and TEMP	Multi-year dynamical prediction system with a high skill in forecasting wildfire probabilities and drought for 10–23 and 10–45 months lead time	The state-of-the-art earth system model and ocean data assimilations show low frequency of rainfall, soil moisture and wildfire probabilities. These results agree with reanalysis data.

Abatzoglou et al. 2018a	Contiguous U.S. (Bailey ecoprovinces)	>40 ha	1992-2015	TEMP, VPD, fuel moisture and WS	Differences in temperature, vapour pressure deficit, fuel moisture and wind speed for large and small lightning- and human-caused wildfires during the initial days of fire activity at ecoregion scales across the U.S.	Higher temperature, vapor pressure deficit and lower 100-hour fuel moisture play the main role in occurrence of large fires of both human and lightening -causes. Wind speed is more positively correlated to large human-caused wildfires compared to other types of fire.
Abatzoglou et al. 2018b	Global	Gridded data	1997-2016	PREC, VPD, and ETo	Patterns of interannual climate-fire relationships	In the regions with weaker correlation between climatic variables and fire activity, fuel moisture shows strong negative correlation with wildfire burned area. On the other hand, precipitation measures conducive to fire season shows strong negative correlation with fire season and burned area in the regions with stronger correlation to climatic variables. Climatic variables only explain 33% of interannual global fire activity.
Turco et al. 2018	Global	Gridded data	1995-2016	SPI, SPEI, and TEMP	- Seasonal forecast of burned area anomalies - Use the standardized precipitation index as the climate predictor for burned area	More accurate climate predictions, yield more accurate global fire activity over the global burnable area (~60%). Through currently available seasonal predictions, the accuracy of fire season forecasts still remains significant in a large portion of globe (~40%).
Viedma et al. 2018	West-central Spain	>1 ha	1979-2008	TEMP, SPEI, CFWI, TOPO and landscape features	The changing role of biophysical and human-related factors on wildfires in a rural area in west-central Spain.	The authors composed various models with different variables. The models with topography, land use and land cover yielded the best accuracy of predicting fire activity. They concluded that other socio-economic, forest interface and climatic variables are minor variables. They also showed that as time went by, wildfires occurred in the less-prone areas and as they spread, they will become more hazardous for humans.
Holden et al. 2018	Western U.S. (forests)	>405 ha	1984-2015	TEMP, RH, and SWE	- Near-surface air temperature and evaporative demand are strongly influenced by moisture availability - Their role in regulating fire activity	The main driver of area burned in the forests of western U.S. is decreased summer rainfall. Considering the interactions of number of wetting days (WRD; days with rainfall ≥2.54 mm), temperature and vapor pressure deficit, the net effect of WRD anomalies on area burned was much greater than those of VPD. Their analyses show that the effects of both VPD and WRD are greater than snowpack on area burned.
Crockett and Westerling 2018	Sierra Nevada	>405 ha	1984-2014	TEMP, PREC, CWD	Impact of droughts on wildfire severity	The authors show that in fire extent and severity are greater during droughts (1984-2014).
Keyser and Westerling 2019	Northern Rocky Mountains, Sierra Nevada Mountains, and Southwest	>405 ha	1984-2014	TEMP, MD, location, TOPO, snowpack condition, and vegetation condition	High severity area burned for the western U.S. and three sub-regions—the Northern Rocky Mountains, Sierra Nevada Mountains, and Southwest	Their model elaborated high fire severity in western U.S. during summers of 1988 to 2002. Moreover, snowpack, vegetation type, location, elevation and spring temperature improved the model accuracy of predicting extreme fire severity in the aforementioned time space.
Joseph et al. 2019	Contiguous U.S.	>400 ha	1984-2016	RH, TEMP, PREC, WS and housing data	Spatiotemporal prediction of wildfire size extremes with Bayesian finite sample maxima	Statistical analyses show that temperature, dryness and housing are the main drivers of extreme wildfires. They influence fire size distribution through affecting fire frequency and size.
Williams et al. 2019	California	>0.1 ha	1972-2018	FM1000, FFWI, SPI, TEMP, WS, VPD, and ETo	Impact of observed climate change on wildfire activity in California	Area burned by wildfires escalated as much as 400% in the space of 1972 and 2018. The most increase of area burned had occurred during summer which is due to warming and dryness.

* Abbreviations:

AFFDI: Australian Forest Fire Danger Index.
BI: Burning Index.
CFWI: Canadian Fire Weather Index.
CSR: Cumulative Severity Rating.
CWD: Climatic Water Deficit.
DMC: Duff Moisture Codes
DP: Dew Point.
L: Elevation.
ERC: Energy Release Component.
ETo: Reference Evapotranspiration.
FD: Fuel Density.
FFMC: Fine Fuel Moisture Code.
FFWI: Fosberg Fire Weather Index.
FM100: 100-hour Fuel Moisture.
FM1000: 1000-hour Fuel Moisture.
FMC: Fuel Moisture Code.
FSI: Fire Severity Index.
HI: Haines Index.
ISI: Initial Spread Index.
KDBI: Keetch-Byram Drought Index.
LFM: Live Fuel Moisture.
MD: Moisture Deficit.
PDSI: Palmer Drought Severity Index.
PET: Potential Evapotranspiration.
PREC: Precipitation.
RH: Relative Humidity.
SDA: Snowmelt Days Anomaly.
SM: Soil Moisture.
SPEI: Standardized Precipitation and Evapotranspiration Index.
SPI: Standardized Precipitation Index.
SWC: Soil Water Content.
SWE: Snow Water Equivalent.
TEMP: Temperature.
TOPO: Topography.
VPD: Vapour Pressure Deficit.
WS: Wind Speed.

Table S2. Overlap and redundancy among fire drivers. The normalized redundancy measure (MacKay 2003) among various combinations of pairs of LFM, Wind, SHI3, FM100, FM1000, ERC, BI, and VPD is presented. The normalized redundancy measure is calculated on the series of these climatic, meteorological and biophysical variables corresponding to all fires. A value of zero corresponds to zero mutual information between the two variables, whereas a value of one is associated with one variable being completely redundant with the knowledge of the other.

	LFM	Wind	SHI3	FM100	FM1000	ERC	BI	VPD
LFM	1	0.35	0.38	0.37	0.38	0.39	0.32	0.37
Wind	0.35	1	0.37	0.38	0.38	0.40	0.33	0.36
SHI3	0.38	0.37	1	0.42	0.43	0.43	0.35	0.42
FM100	0.37	0.38	0.42	1	0.46	0.48	0.40	0.43
FM1000	0.38	0.38	0.43	0.46	1	0.51	0.41	0.43
ERC	0.39	0.40	0.43	0.48	0.51	1	0.42	0.43
BI	0.32	0.33	0.35	0.40	0.41	0.42	1	0.36
VPD	0.37	0.36	0.42	0.43	0.43	0.43	0.36	1

Table S3. Pearson correlation coefficients (r) and associated p-values between drivers and fire sizes of different categories.

Fire Size (ha)	Pearson Correlation															
	LFM		Wind		SHI3		FM100		FM1000		ERC		BI		VPD	
	r	p	r	p	r	p	r	p	r	p	r	p	r	p	r	p
0	-0.01563	3.00E-03	0.04086	3.95E-08	0.02168	3.98E-05	-0.03146	2.47E-09	-0.02564	1.18E-06	0.03332	2.67E-10	0.03957	6.27E-14	0.03223	9.98E-10
2	-0.04192	1.00E-02	0.11789	4.08E-08	0.06046	0.00018	-0.08493	1.42E-07	-0.07175	8.83E-06	0.08829	4.45E-08	0.10464	8.54E-11	0.06673	3.59E-05
4	-0.04708	2.00E-02	0.14259	1.13E-08	0.06901	0.00039	-0.09526	9.47E-07	-0.0794	4.44E-05	0.09812	4.41E-07	0.11718	1.57E-09	0.07479	0.00012
40	-0.07105	3.00E-02	0.19127	8.16E-07	0.09586	0.0033	-0.12704	9.56E-05	-0.10103	0.00195	0.1293	7.14E-05	0.14867	4.81E-06	0.09416	0.0039
120	-0.09517	3.00E-02	0.21481	2.13E-05	0.10646	0.01495	-0.14231	0.00111	-0.11121	0.011	0.14219	0.00112	0.165	0.00015	0.09896	0.02375
405	-0.10792	8.00E-02	0.24236	0.00029	0.13044	0.03028	-0.17906	0.00283	-0.15194	0.01149	0.17757	0.00307	0.18118	0.00252	0.12788	0.03371
2025	-0.13569	1.80E-01	0.20847	0.04493	0.12268	0.20807	-0.16533	0.08879	-0.15092	0.12073	0.18793	0.05256	0.1564	0.10768	0.13743	0.15808

Table S4. Kendall correlation coefficients (r) and associated p-values between drivers and fire sizes of different categories.

Fire Size (ha)	Kendall Correlation															
	LFM		Wind		SHI3		FM100		FM1000		ERC		BI		VPD	
	r	p	r	p	r	p	r	p	r	p	r	p	r	p	r	p
0	0.00165	0.67067	9.66E-06	0.99859	0.01218	0.0014	-0.0162	2.12E-05	-0.00285	0.45533	0.02638	4.46E-12	0.03996	1.04E-25	0.10561	5.33E-169
2	-0.04937	1.10E-05	0.10447	7.79E-13	0.05044	4.53E-06	-0.11352	5.66E-25	-0.09721	9.73E-19	0.10892	4.06E-23	0.1153	1.04E-25	0.10157	2.59E-20
4	-0.03469	0.00994	0.10607	3.52E-10	0.05672	1.64E-05	-0.11465	3.06E-18	-0.09346	1.25E-12	0.10579	9.26E-16	0.11909	1.49E-19	0.10906	1.19E-16
40	-0.03436	0.12726	0.09777	0.00019	0.06241	0.00443	-0.10965	5.72E-07	-0.08251	0.00017	0.10841	7.65E-07	0.14297	7.05E-11	0.09205	2.69E-05
120	-0.0832	0.00601	0.11616	0.00068	0.05273	0.07221	-0.09561	0.00111	-0.05598	0.05628	0.08896	0.00242	0.14636	6.03E-07	0.04561	0.11991
405	-0.09414	0.02469	0.13319	0.00338	0.09609	0.01748	-0.19221	1.99E-06	-0.14823	0.00025	0.16612	3.97E-05	0.22183	4.09E-08	0.06636	0.10078
2025	-0.11562	0.09472	0.11245	0.11115	0.03687	0.57552	-0.15117	0.0212	-0.16282	0.01306	0.18116	0.00574	0.15294	0.01974	0.13318	0.04238

Table S5. Spearman correlation coefficients (r) and associated p-values between drivers and fire sizes of different categories.

Fire Size (ha)	Spearman Correlation															
	LFM		Wind		SHI3		FM100		FM1000		ERC		BI		VPD	
	r	p	r	p	r	p	r	p	r	p	r	p	r	p	r	p
0	0.00246	0.64717	-0.0005	0.94675	0.01684	0.00141	-0.0222	2.58E-05	-0.00323	0.53997	0.03601	8.74E-12	0.05454	4.45E-25	0.14583	6.57E-170
2	-0.07213	1.13E-05	0.15189	1.37E-12	0.07406	4.48E-06	-0.16604	4.52E-25	-0.14196	1.08E-18	0.15936	3.37E-23	0.16801	1.22E-25	0.14836	2.74E-20
4	-0.05086	0.01032	0.15399	6.73E-10	0.08319	1.88E-05	-0.16774	4.16E-18	-0.13739	1.36E-12	0.15544	9.71E-16	0.17464	1.62E-19	0.16097	8.82E-17
40	-0.05065	0.12979	0.14315	0.00024	0.09243	0.00461	-0.16248	5.65E-07	-0.12306	0.00016	0.16332	4.93E-07	0.21288	4.49E-11	0.13768	2.32E-05
120	-0.12358	0.00595	0.17243	0.00068	0.07973	0.06872	-0.14213	0.00113	-0.08444	0.05384	0.13387	0.00218	0.22016	3.77E-07	0.06823	0.119461772
405	-0.13785	0.02623	0.19933	0.00305	0.14113	0.01899	-0.28513	1.47E-06	-0.21815	0.00026	0.24718	3.29E-05	0.33388	1.30E-08	0.09983	0.097914209
2025	-0.15699	0.12264	0.16868	0.10602	0.04998	0.6092	-0.21955	0.02308	-0.22667	0.01888	0.25987	0.00687	0.21633	0.02522	0.19192	0.047662947

Table S6. Ten representative fires with their drivers. These are relatively large (>100 ha) to large (>405 ha) fires that are driven by the concurrence of non-extreme but critical variables. These drivers are not extreme individually, but when combined created the extreme impact. The critical thresholds for all drivers are provided for comparison. Divergence from critical threshold values (Δ) are calculated as the driver value minus the threshold. For clarity, the delta-values that shows the driver is not critical are shown in red. While these values are not extreme, concurrence of at least two critical drivers caused fire growth.

#	Fire Name	Latitude	Longitude	Date	Fire Size (ha)	LFM (%)	Wind (m/sec)	SHI3	FM100 (%)	FM1000 (%)	ERC (kJ/m2)	BI	VPD (kPa)	Δ LFM	Δ Wind	Δ SHI3	Δ FM 100	Δ FM 1000	Δ ERC	Δ BI	Δ VPD
1	ALISO	33.442	-117.394	21-Mar-02	971.25	142.46	2.73	-0.18	10.84	12.97	568.21	36.62	0.95	54.06	0.43	0.09	1.44	0.47	-49.79	-6.68	-0.55
2	ANTONIO	33.592	-117.617	13-May-02	595.7	98	3.62	0.35	11.2	14.13	534.73	38.58	1.64	9.6	1.32	0.62	1.8	1.63	-83.27	-4.72	0.14
3	OTAY 28	32.585	-116.835	15-Apr-96	567.37	139.41	0.46	0.28	11.16	14.92	507.99	32.16	1.6	51.01	-1.84	0.55	1.76	2.42	-110.01	-11.14	0.1
4	EVENING	33.869	-117.684	21-Apr-02	360.98	108.05	2.83	-0.94	11.72	12.75	557.88	35.6	0.93	19.65	0.53	-0.67	2.32	0.25	-60.12	-7.7	-0.57
5	NICHOLS	33.717	-117.351	2-Jul-95	343.98	90	3.31	-0.37	10.96	13.09	572.8	40.5	1.92	1.6	1.01	-0.1	1.56	0.59	-45.2	-2.8	0.42
6	PEDLEY	34.021	-117.481	12-May-10	290.04	89	3.37	-1.4	12.17	13.32	566.03	41.84	1.39	0.6	1.07	-1.13	2.77	0.82	-51.97	-1.46	-0.11
7	YSABEL	33.085	-116.883	13-Jun-92	263.05	86	3.62	-0.39	14.48	15.35	427.44	30.76	1.17	-2.4	1.32	-0.12	5.08	2.85	-190.56	-12.54	-0.33
8	BANNER	33.063	-116.554	9-Jun-99	199.51	90	3.86	-0.86	9.28	11.9	644.99	51.22	1.32	1.6	1.56	-0.59	-0.12	-0.6	26.99	7.92	-0.18
9	SHOOTING	34.31	-118.367	1-May-97	194.25	90	3.93	-0.04	9.77	9.38	744.71	51.39	1.43	1.6	1.63	0.23	0.37	-3.12	126.71	8.09	-0.07
10	166	34.964	-119.842	12-Jul-11	140.43	86.04	0.83	-0.58	8.46	10.11	729.12	48.16	1.68	-2.36	-1.47	-0.31	-0.94	-2.39	111.12	4.86	0.18
		Critical Values				**88.4**	**2.3**	**-0.27**	**9.4**	**12.5**	**618**	**43.3**	**1.5**								

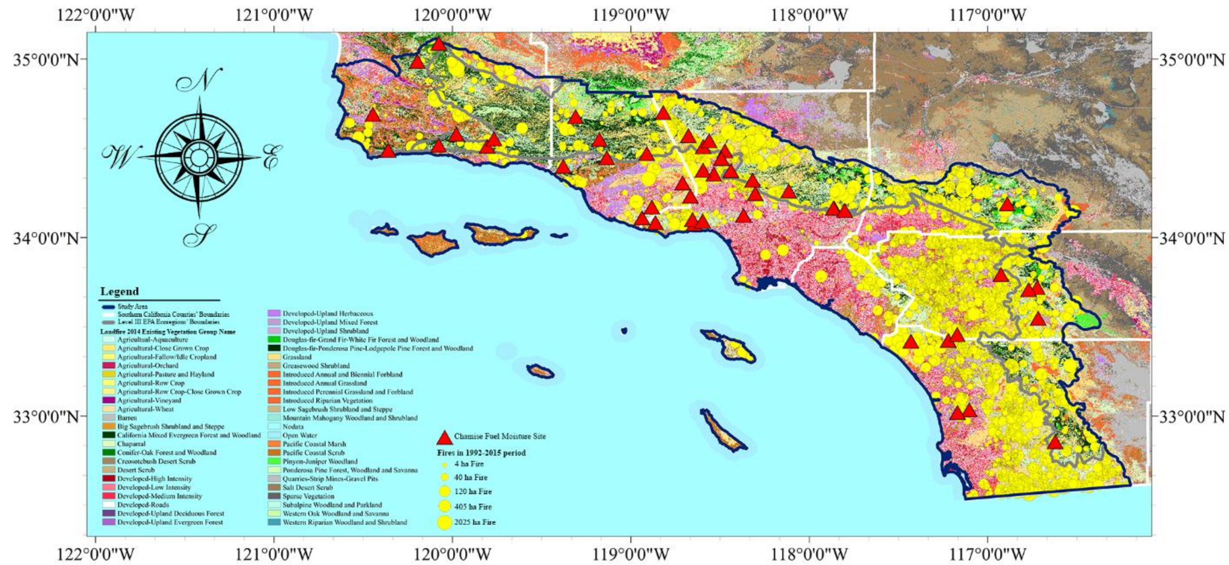

Figure S1. Geographic location of the study region. The boundaries of the region (blue line not including the islands), the Southern California counties (white line) and Level III EPA ecoregions 8 and 85 (gray line; Omernik 1987) are shown. The distribution of vegetation cover (LNADFIRE, 2014) and the location of chamise fuel moisture measurement sites between 1979 and 2017 (red triangles; USFS 2018) and the location and size of wildfires during 1992 to 2015 (yellow circles; Short 2017) are also depicted.

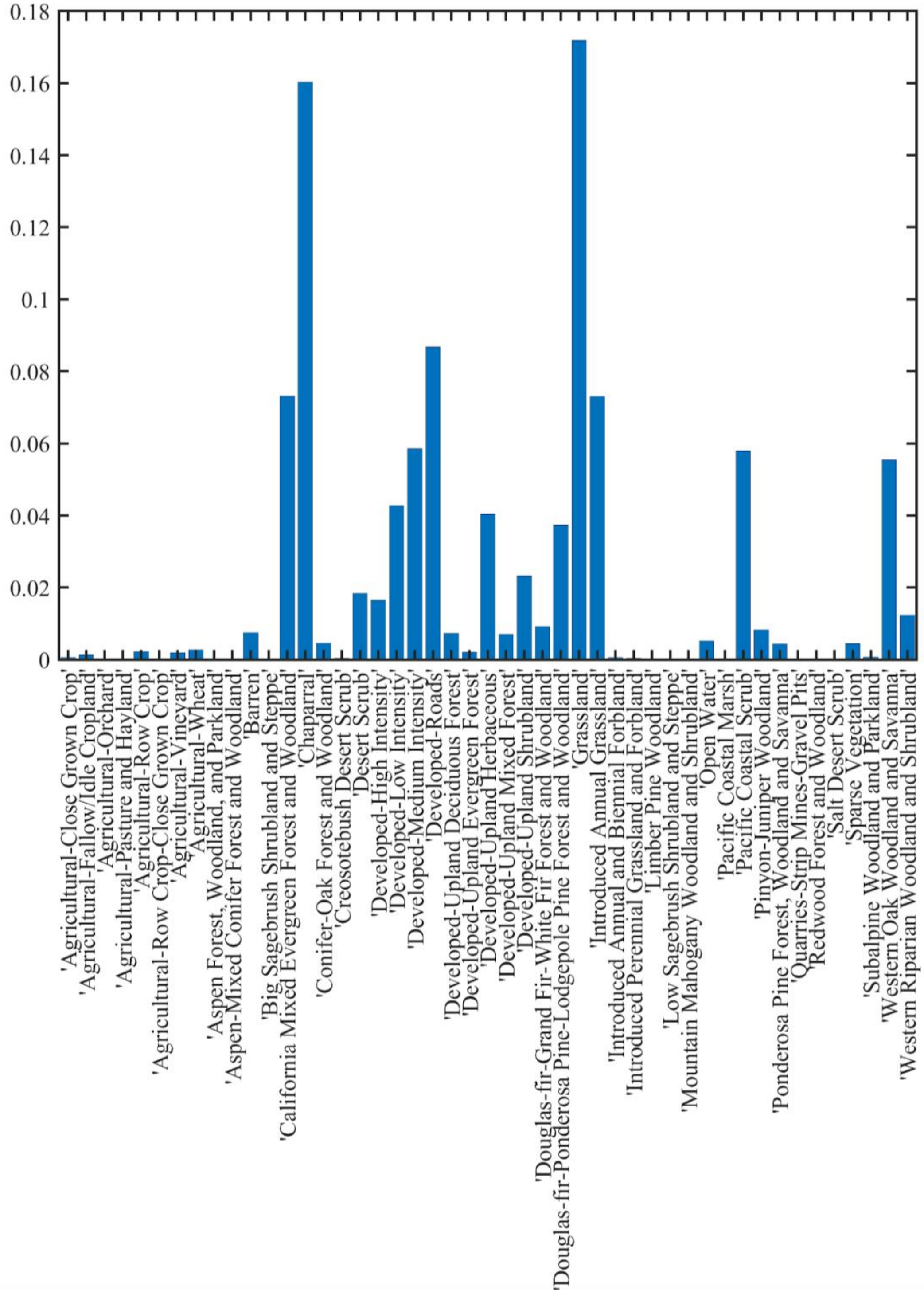

Figure S2. Histogram of vegetation type frequency in the study area. Chaparral and grassland are the dominant vegetation types in coastal southern California. Y-axis represents fraction of area occupied by each vegetation type.

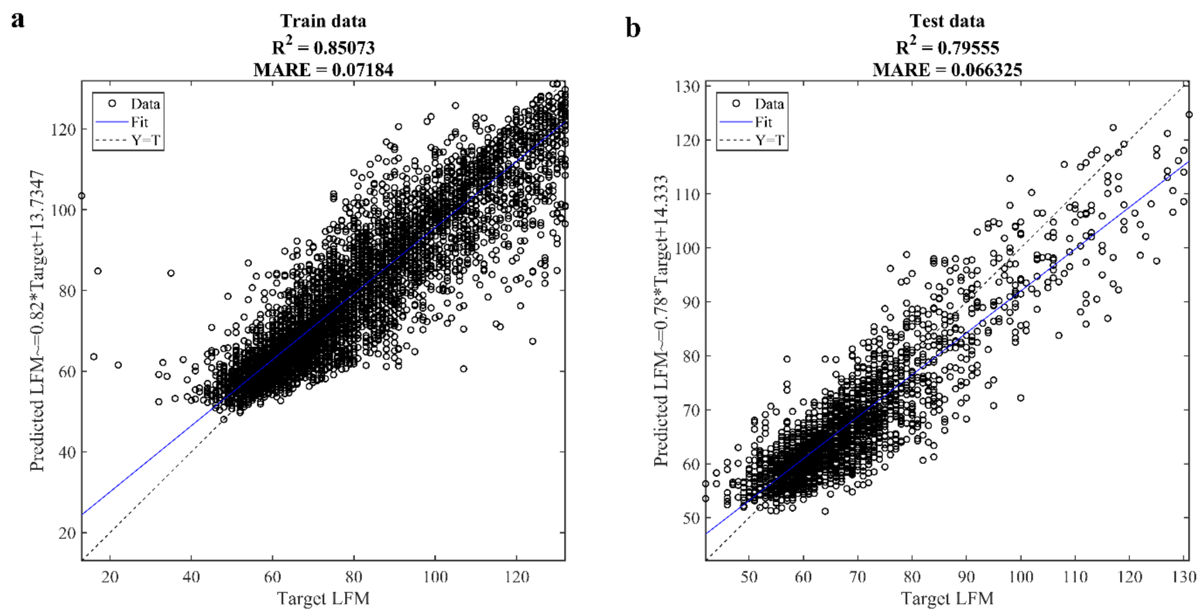

Figure S3. Performance of the Support Vector Regression. SVR model (Drucker et al. 1997) model is used to create the gridded LFM dataset. Black dots represent observed LFM values (x-axis) versus modelled LFM values (y-axis) for the train data (75% of all available data) and the test data (the remaining 25% of the available data). The selected SVR model yields R^2=0.85 and MARE=0.07 for train and R^2=0.8 and MARE=0.066 for test stages.

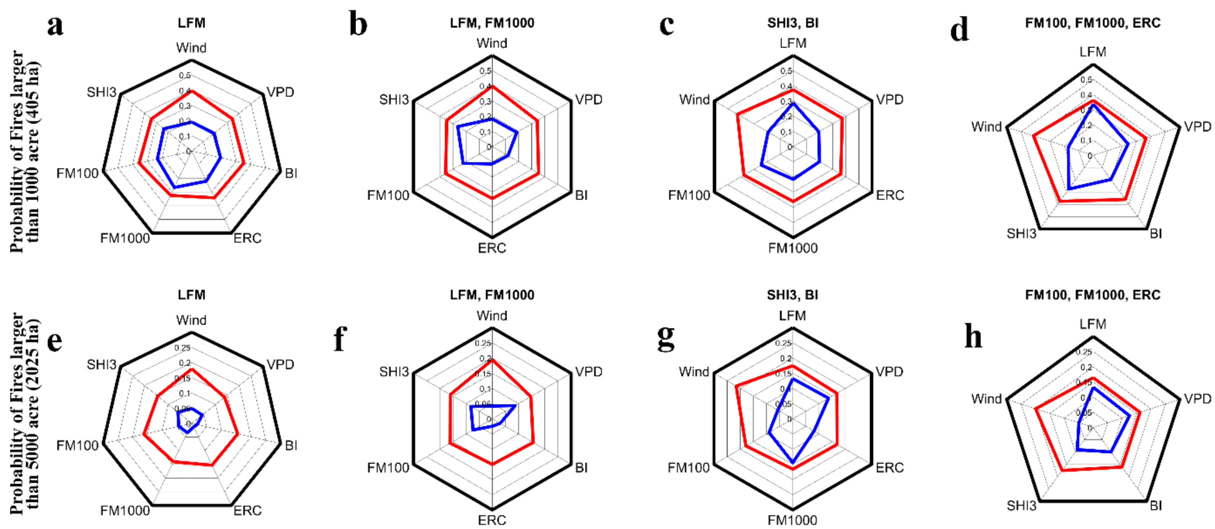

Figure S4. Compounding effects of multiple drivers grow fire sizes. Probabilities of observing **a)** large (>405 ha) and **e)** very large (>2025 ha) fires when various drivers are critical (red line) and not critical (blue line). Probabilities of observing large (>405 ha) fires when various drivers are critical (red) and not critical (blue) *given* **b)** *LFM and FM100*, **c)** *SHI3 and BI, and* **d)** *FM100, FM1000 and ERC are critical*. Probabilities of observing very large (>2025 ha) fires when various drivers are critical (red) and not critical (blue) *given* **f)** *LFM and FM100*, **g)** *SHI3 and BI, and* **h)** *FM100, FM1000 and ERC are critical*. Only fires of larger than 40 ha (100 acre) are used in this analysis.

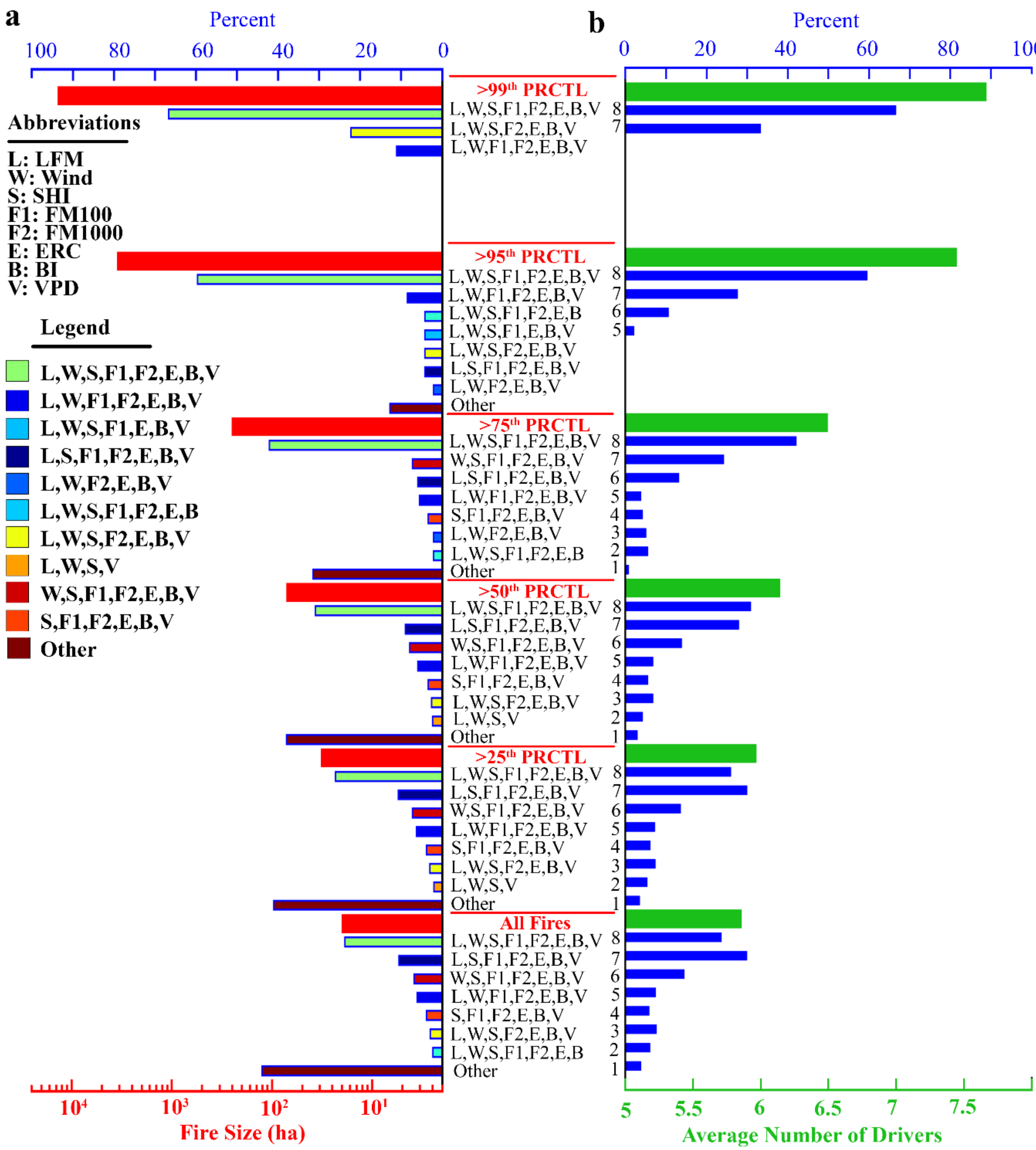

Figure S5. Concurrence of critical conditions of drivers for fires of different size categories in the study region between 1992 and 2015. Only fires of larger than 40 ha (100 acre) are included in the analysis. Top x-axis shows percentage of fires in each size category observing concurrence of critical conditions of the drivers described in the middle panel. Fire size categories include: larger than 0th percentile (100 acre; 40 ha), 25th, 50th, 75th, 95th, and 99th percentiles of all fires larger than 40 ha. **a)** Concurrence of critical conditions of certain drivers explained in the middle panel creates the fires, and **b)** Number of critical drivers for fires of each category.

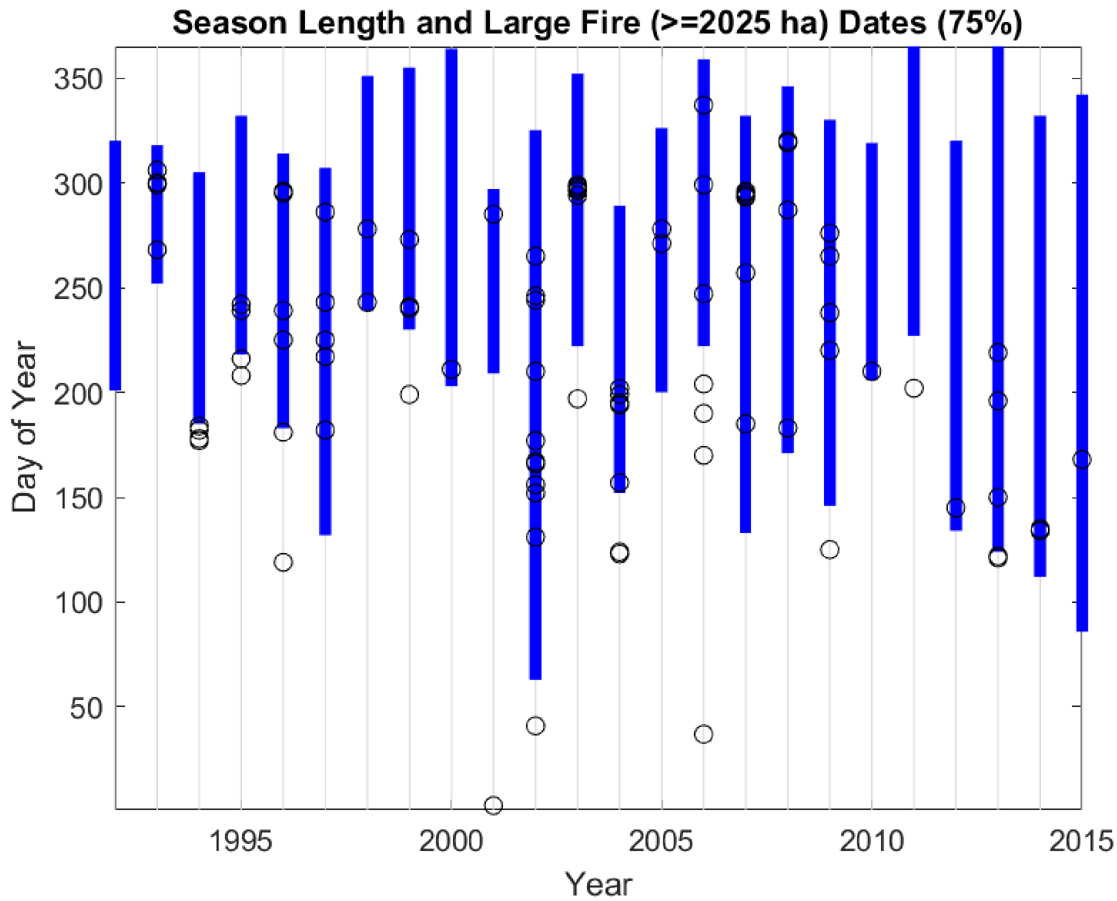

Figure S6. Megafire season (the interval between the first and the last day of the year that all drivers were critical in 75% of all the grid cells) between 1992 and 2015. The circles show the large fires' (>=2025 ha) discovery date (day of the year).

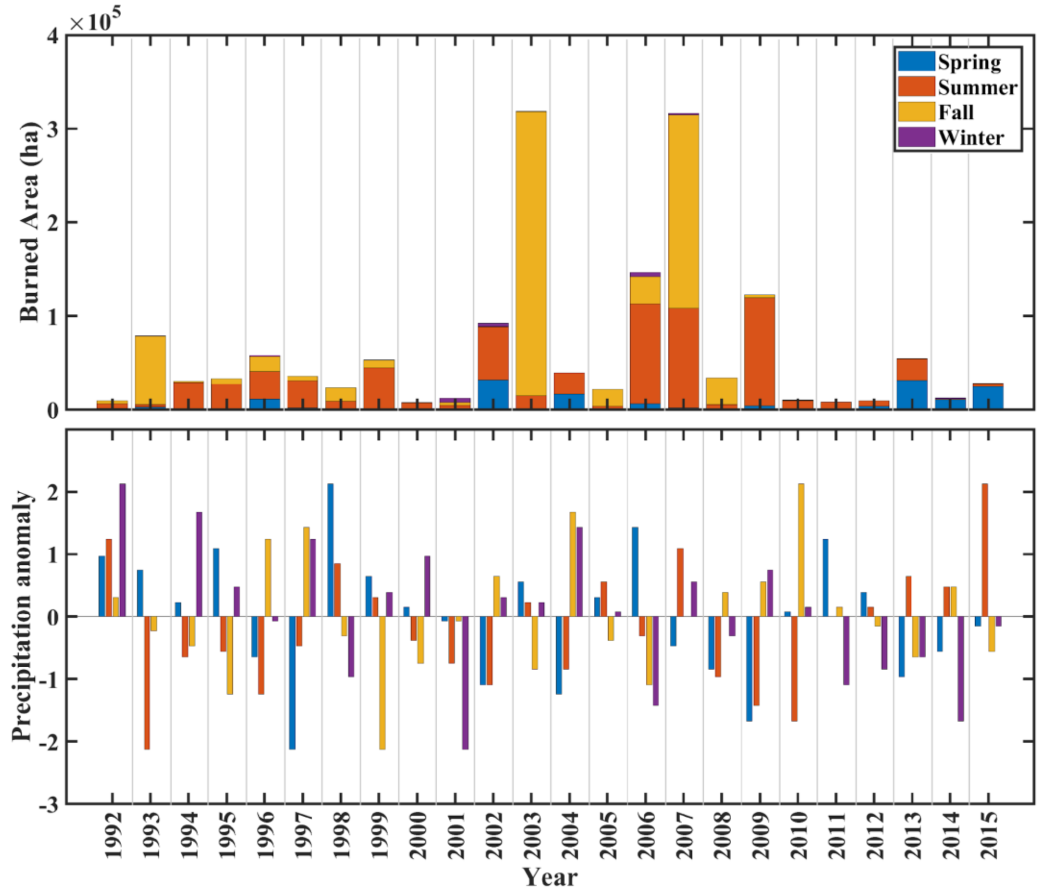

Figure S7. Seasonal cumulative fire size and normalized precipitation anomaly between 1992 and 2015. Extreme fall fire season is associated with above normal precipitation in spring and below normal precipitation in summer.

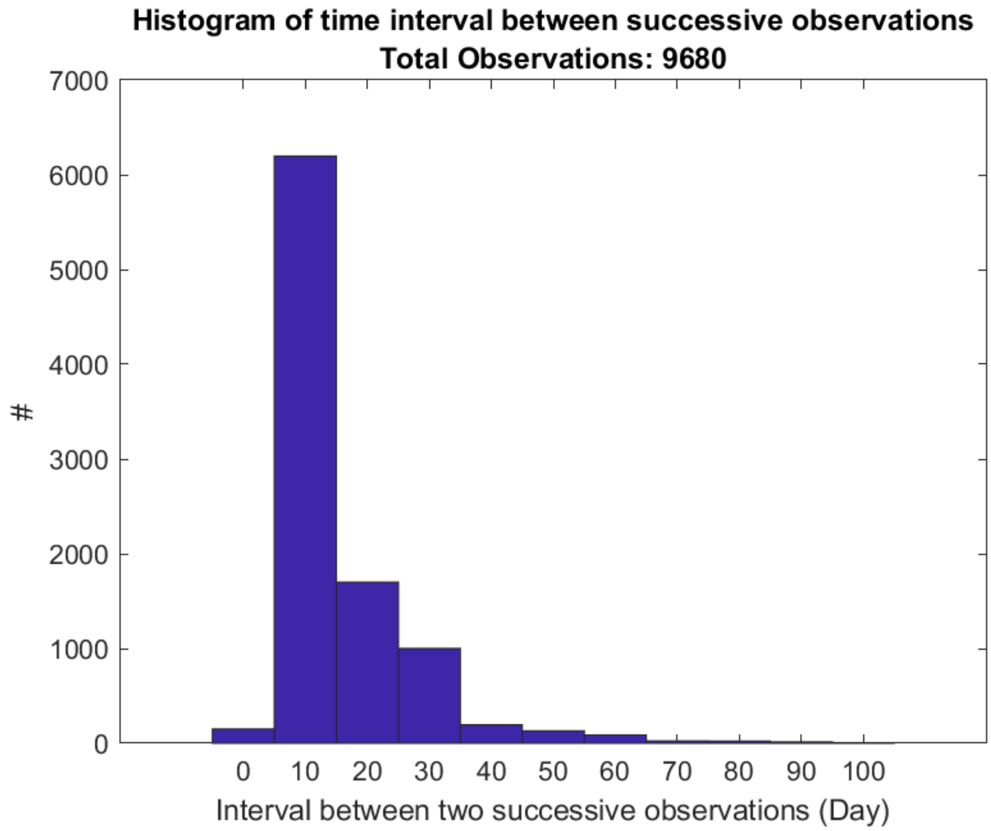

Figure S8. Distribution of temporal lags between successive observations of LFM. U.S. Forest Service's (USFS) National Fuel Moisture Database (NFMD 2018) provide 9,680 records of chamise fuel moisture measurements between 1983 and 2017 from 51 chamise fuel moisture sites in Southern California. Most of the successive measurements at each site were performed within 10 to 20 days interval.

References

Abatzoglou, J.T. and Kolden, C.A., 2011. Climate change in western US deserts: potential for increased wildfire and invasive annual grasses. Rangeland Ecology & Management, 64(5), pp.471-478.

Abatzoglou, J.T., 2013. Development of gridded surface meteorological data for ecological applications and modelling. *International Journal of Climatology*, *33*(1), pp.121-131.

Abatzoglou, J.T. and Kolden, C.A., 2013. Relationships between climate and macroscale area burned in the western United States. International Journal of Wildland Fire, 22(7), pp.1003-1020.

Abatzoglou, J.T. and Williams, A.P., 2016. Impact of anthropogenic climate change on wildfire across western US forests. Proceedings of the National Academy of Sciences, 113(42), pp.11770-11775.

Abatzoglou, J.T., Balch, J.K., Bradley, B.A. and Kolden, C.A., 2018a. Human-related ignitions concurrent with high winds promote large wildfires across the USA. International Journal of Wildland Fire, 27(6), pp.377-386.

Abatzoglou, J.T., Kolden, C.A., Balch, J.K. and Bradley, B.A., 2016. Controls on interannual variability in lightning-caused fire activity in the western US. Environmental Research Letters, 11(4), p.045005.

Abatzoglou, J.T., Williams, A.P., Boschetti, L., Zubkova, M. and Kolden, C.A., 2018b. Global patterns of interannual climate–fire relationships. Global change biology, 24(11), pp.5164-5175.

Balch, J.K., Bradley, B.A., Abatzoglou, J.T., Nagy, R.C., Fusco, E.J. and Mahood, A.L., 2017. Human-started wildfires expand the fire niche across the United States. Proceedings of the National Academy of Sciences, 114(11), pp.2946-2951.

Barbero, R., Abatzoglou, J.T., Kolden, C.A., Hegewisch, K.C., Larkin, N.K. and Podschwit, H., 2015a. Multi-scalar influence of weather and climate on very large-fires in the Eastern United States. International Journal of Climatology, 35(8), pp.2180-2186.

Barbero, R., Abatzoglou, J.T., Larkin, N.K., Kolden, C.A. and Stocks, B., 2015b. Climate change presents increased potential for very large fires in the contiguous United States. International Journal of Wildland Fire, 24(7), pp.892-899.

Barbero, R., Abatzoglou, J.T., Steel, E.A. and Larkin, N.K., 2014. Modeling very large-fire occurrences over the continental United States from weather and climate forcing. Environmental research letters, 9(12), p.124009.

Bessie, W.C. and Johnson, E.A., 1995. The relative importance of fuels and weather on fire behavior in subalpine forests. Ecology, 76(3), pp.747-762.

Brown, T.J., Hall, B.L. and Westerling, A.L., 2004. The impact of twenty-first century climate change on wildland fire danger in the western United States: an applications perspective. Climatic change, 62(1-3), pp.365-388.

Chikamoto, Y., Timmermann, A., Widlansky, M.J., Balmaseda, M.A. and Stott, L., 2017. Multi-year predictability of climate, drought, and wildfire in southwestern North America. Scientific reports, 7(1), p.6568.

Crockett, J.L. and Westerling, A.L., 2018. Greater temperature and precipitation extremes intensify Western US droughts, wildfire severity, and Sierra Nevada tree mortality. Journal of Climate, 31(1), pp.341-354. (12)

Deeming, J.E., Burgan, R.E. and Cohen, J.D., 1977. *The national fire-danger rating system--1978* (Vol. 39). Intermountain Forest and Range Experiment Station, Forest Service, US Department of Agriculture.

Dennison, P.E. and Moritz, M.A., 2009. Critical live fuel moisture in chaparral ecosystems: a threshold for fire activity and its relationship to antecedent precipitation. International Journal of Wildland Fire, 18(8), pp.1021-1027.

Dennison, P.E., Brewer, S.C., Arnold, J.D. and Moritz, M.A., 2014. Large wildfire trends in the western United States, 1984–2011. Geophysical Research Letters, 41(8), pp.2928-2933.

Dillon, G.K., Holden, Z.A., Morgan, P., Crimmins, M.A., Heyerdahl, E.K. and Luce, C.H., 2011. Both topography and climate affected forest and woodland burn severity in two regions of the western US, 1984 to 2006. Ecosphere, 2(12), pp.1-33.

Drucker, H., Burges, C.J., Kaufman, L., Smola, A.J. and Vapnik, V., 1997. Support vector regression machines. In Advances in neural information processing systems (pp. 155-161).

Finney, M.A., McHugh, C.W., Grenfell, I.C., Riley, K.L. and Short, K.C., 2011. A simulation of probabilistic wildfire risk components for the continental United States. Stochastic Environmental Research and Risk Assessment, 25(7), pp.973-1000.
Fischer, H., Schüpbach, S., Gfeller, G., Bigler, M., Röthlisberger, R., Erhardt, T., Stocker, T.F., Mulvaney, R. and Wolff, E.W., 2015. Millennial changes in North American wildfire and soil activity over the last glacial cycle. Nature geoscience, 8(9), p.723.
Flannigan, M., Cantin, A.S., De Groot, W.J., Wotton, M., Newbery, A. and Gowman, L.M., 2013. Global wildland fire season severity in the 21st century. Forest Ecology and Management, 294, pp.54-61.
Hanes, T.L., 1977. California chaparral.
Holden, Z.A., Luce, C.H., Crimmins, M.A. and Morgan, P., 2011. Wildfire extent and severity correlated with annual streamflow distribution and timing in the Pacific Northwest, USA (1984–2005). Ecohydrology, 5(5), pp.677-684.
Holden, Z.A., Swanson, A., Luce, C.H., Jolly, W.M., Maneta, M., Oyler, J.W., Warren, D.A., Parsons, R. and Affleck, D., 2018. Decreasing fire season precipitation increased recent western US forest wildfire activity. Proceedings of the National Academy of Sciences, 115(36), pp.E8349-E8357.
InciWeb, 2019. https://inciweb.nwcg.gov/incident/5670/. Last retrieved on June 3, 2019.
Jin, Y., Randerson, J.T., Faivre, N., Capps, S., Hall, A. and Goulden, M.L., 2014. Contrasting controls on wildland fires in Southern California during periods with and without Santa Ana winds. Journal of Geophysical Research: Biogeosciences, 119(3), pp.432-450.
Jolly, W.M., Cochrane, M.A., Freeborn, P.H., Holden, Z.A., Brown, T.J., Williamson, G.J. and Bowman, D.M., 2015. Climate-induced variations in global wildfire danger from 1979 to 2013. Nature communications, 6, p.7537.
Joseph, M.B., Rossi, M.W., Mietkiewicz, N.P., Mahood, A.L., Cattau, M.E., St. Denis, L.A., Nagy, R.C., Iglesias, V., Abatzoglou, J.T. and Balch, J.K., 2019. Spatiotemporal prediction of wildfire size extremes with Bayesian finite sample maxima. Ecological Applications, p.e01898.
Keyser, A.R. and Westerling, A.L., 2019. Predicting increasing high severity area burned for three forested regions in the western United States using extreme value theory. Forest Ecology and Management, 432, pp.694-706.
LANDFIRE, 2018. https://www.landfire.gov/evt.php. Last retrieved on May 4, 2019.
Littell, J.S., McKenzie, D., Peterson, D.L. and Westerling, A.L., 2009. Climate and wildfire area burned in western US ecoprovinces, 1916–2003. Ecological Applications, 19(4), pp.1003-1021.
Liu, Y., Goodrick, S.L. and Stanturf, J.A., 2013. Future US wildfire potential trends projected using a dynamically downscaled climate change scenario. Forest Ecology and Management, 294, pp.120-135.
Liu, Y., Stanturf, J. and Goodrick, S., 2010. Trends in global wildfire potential in a changing climate. Forest ecology and management, 259(4), pp.685-697.
Luo, L., Tang, Y., Zhong, S., Bian, X. and Heilman, W.E., 2013. Will future climate favor more erratic wildfires in the Western United States?. Journal of Applied Meteorology and Climatology, 52(11), pp.2410-2417.
MacKay, David J.C., 2003. "2.4 Definition of entropy and related functions". Information Theory, Inference, and Learning Algorithms. Cambridge University Press. p. 33. ISBN 0-521-64298-1.

NARR, 2018. A long-term, consistent, high-resolution climate dataset for the North American domain, as a major improvement upon the earlier global reanalysis datasets in both resolution and accuracy, Fedor Mesinger et al., submitted to BAMS 2004. https://www.esrl.noaa.gov/psd/. Last retrieved on May 4, 2019.

NFMD, 2018. https://www.wfas.net/nfmd/public/index.php. Last retrieved on May 4, 2019.

Omernik, J.M. 1987. Ecoregions of the conterminous United States. Map (scale 1:7,500,000). Annals of the Association of American Geographers 77(1):118-125.

Parisien, M.A., Snetsinger, S., Greenberg, J.A., Nelson, C.R., Schoennagel, T., Dobrowski, S.Z. and Moritz, M.A., 2012. Spatial variability in wildfire probability across the western United States. International Journal of Wildland Fire, 21(4), pp.313-327.

Pivovaroff, A.L., Emery, N., Sharifi, M.R., Witter, M., Keeley, J.E. and Rundel, P.W., 2019. The effect of ecophysiological traits on live fuel moisture content. *Fire*, *2*(2), p.28.

PRISM, 2018. http://www.prism.oregonstate.edu. Last retrieved on May 4, 2019.

Raei, E., Nikoo, M.R., AghaKouchak, A., Mazdiyasni, O. and Sadegh, M., 2018. GHWR, a multi-method global heatwave and warm-spell record and toolbox. *Scientific data*, *5*(1), pp.1-15.

Raphael, M.N., 2003. The santa ana winds of california. *Earth Interactions*, *7*(8), pp.1-13.

Riley, K.L., Abatzoglou, J.T., Grenfell, I.C., Klene, A.E. and Heinsch, F.A., 2013. The relationship of large fire occurrence with drought and fire danger indices in the western USA, 1984–2008: the role of temporal scale. International Journal of Wildland Fire, 22(7), pp.894-909.

Schoennagel, T., Balch, J.K., Brenkert-Smith, H., Dennison, P.E., Harvey, B.J., Krawchuk, M.A., Mietkiewicz, N., Morgan, P., Moritz, M.A., Rasker, R. and Turner, M.G., 2017. Adapt to more wildfire in western North American forests as climate changes. Proceedings of the National Academy of Sciences, 114(18), pp.4582-4590.

Short, Karen C. 2017. Spatial wildfire occurrence data for the United States, 1992-2015 [FPA_FOD_20170508]. 4th Edition. Fort Collins, CO: Forest Service Research Data Archive. https://doi.org/10.2737/RDS-2013-0009.4.

Spracklen, D.V., Mickley, L.J., Logan, J.A., Hudman, R.C., Yevich, R., Flannigan, M.D. and Westerling, A.L., 2009. Impacts of climate change from 2000 to 2050 on wildfire activity and carbonaceous aerosol concentrations in the western United States. Journal of Geophysical Research: Atmospheres, 114(D20).

Stavros, E.N., Abatzoglou, J.T., McKenzie, D. and Larkin, N.K., 2014. Regional projections of the likelihood of very large wildland fires under a changing climate in the contiguous Western United States. Climatic Change, 126(3-4), pp.455-468.

Taufik, M., Torfs, P.J., Uijlenhoet, R., Jones, P.D., Murdiyarso, D. and Van Lanen, H.A., 2017. Amplification of wildfire area burnt by hydrological drought in the humid tropics. Nature Climate Change, 7(6), p.428. (33)

Turco, M., Jerez, S., Doblas-Reyes, F.J., AghaKouchak, A., Llasat, M.C. and Provenzale, A., 2018. Skilful forecasting of global fire activity using seasonal climate predictions. Nature communications, 9(1), p.2718.

Viedma, O., Urbieta, I.R. and Moreno, J.M., 2018. Wildfires and the role of their drivers are changing over time in a large rural area of west-central Spain. Scientific reports, 8(1), p.17797.

Westerling, A.L. and Bryant, B.P., 2008. Climate change and wildfire in California. Climatic Change, 87(1), pp.231-249.

Westerling, A.L., 2016. Increasing western US forest wildfire activity: sensitivity to changes in the timing of spring. Philosophical Transactions of the Royal Society B: Biological Sciences, 371(1696), p.20150178.

Westerling, A.L., Bryant, B.P., Preisler, H.K., Holmes, T.P., Hidalgo, H.G., Das, T. and Shrestha, S.R., 2011a. Climate change and growth scenarios for California wildfire. Climatic Change, 109(1), pp.445-463.

Westerling, A.L., Gershunov, A., Brown, T.J., Cayan, D.R. and Dettinger, M.D., 2003. Climate and wildfire in the western United States. Bulletin of the American Meteorological Society, 84(5), pp.595-604.

Westerling, A.L., Hidalgo, H.G., Cayan, D.R. and Swetnam, T.W., 2006. Warming and earlier spring increase western US forest wildfire activity. science, 313(5789), pp.940-943.

Westerling, A.L., Turner, M.G., Smithwick, E.A., Romme, W.H. and Ryan, M.G., 2011b. Continued warming could transform Greater Yellowstone fire regimes by mid-21st century. Proceedings of the National Academy of Sciences, 108(32), pp.13165-13170.

Williams, A.P., Abatzoglou, J.T., Gershunov, A., Guzman-Morales, J., Bishop, D.A., Balch, J.K., Lettenmaier, D.P., 2019. Observed impacts of anthropogenic climate change on wildfire in California. Earth's Future, in press.

Williams, A.P., Seager, R., Macalady, A.K., Berkelhammer, M., Crimmins, M.A., Swetnam, T.W., Trugman, A.T., Buenning, N., Noone, D., McDowell, N.G. and Hryniw, N., 2015. Correlations between components of the water balance and burned area reveal new insights for predicting forest fire area in the southwest United States. International Journal of Wildland Fire, 24(1), pp.14-26.

Yue, X., Mickley, L.J., Logan, J.A. and Kaplan, J.O., 2013. Ensemble projections of wildfire activity and carbonaceous aerosol concentrations over the western United States in the mid-21st century. Atmospheric Environment, 77, pp.767-780.